

A Circle-preserving Subdivision Scheme Based on Local Algebraic Fits

Pavel Chalmovianský^a and Bert Jüttler^b

^aSpezialforschungsbereich SFB013, ^b Department of Applied Geometry

Johannes Kepler University

Linz, Austria

email: pavel.chalmoviansky@jku.at, bert.juettler@jku.at

Abstract—We describe a new method for constructing a sequence of refined polygons, which starts with a sequence of points and associated normals. The newly generated points are sampled from circles which approximate adjacent points and the corresponding normals. By iterating the refinement procedure, we get a limit curve interpolating the data. We show that the limit curve is G^1 , and that it reproduces circles. The method is invariant with respect to group of Euclidean similarities (including rigid transformations and scaling). We also discuss an experimental setup for a G^2 construction and various possible extensions of the method.

Index Terms—subdivision techniques, fitting of algebraic curves

I. INTRODUCTION

During the last years, iterative techniques for generating curve and surfaces have attracted a lot of attention, and they are now frequently being used in Computer Graphics and related areas. The classical linear schemes produce affinely invariant classes of curves and surfaces [1]. They are often obtained by generalizing the subdivision algorithms for certain spline functions, including trigonometric ones [2]. These techniques also included Hermite subdivision schemes, dealing with points with associated derivatives, see [3] and the references cited therein. Recently, several non-linear schemes have emerged, but these schemes – which seem to be promising – are much harder to analyze [4], [5].

On the other hand, various circle-based and circle-preserving techniques for generating curves are available [6], [7], [8], [9]. Due to its technical importance, the reproduction of circular shapes is a desirable feature of constructions for planar curves.

We present a novel non-linear subdivision technique, which is able to reproduce circles. Starting with a sequence of points and associated normals, we compute a circle fit to any two neighboring

points. Then, the new point is picked from this circle. It is shown that the circle is unique, and that the scheme produces G^1 limit curves for certain reasonable classes of input configurations.

The construction can be modified in several ways, including different weights in the objective function used for the fitting, change of the fitted curve, and different strategies of choosing the new point. In particular, we propose a scheme which has experimentally been demonstrated to generate G^2 curves.

The paper is organized as follows. In section 2 we introduce the notation and several necessary notions. Section 3 analyzes the basic step repeated during the refinement – the fitting of the circle to point and normal data. In section 4, we recall the setup for subdivision of curves and adapt it to our construction. Section 5 provides the proof of several facts about the limit curve produced. The last section concludes the paper with several remarks concerning possible variations and improvements of the method.

II. PRELIMINARIES

Let $P = \{\mathbf{p}_0, \dots, \mathbf{p}_n\}$ be a sequence of points, where $\mathbf{p}_i \in \mathbb{R}^2$ for $i = 0, \dots, n$. and $V = \{\vec{\mathbf{n}}_0, \dots, \vec{\mathbf{n}}_n\}$ be a sequence of associated unit vectors, where $\vec{\mathbf{n}}_i = (\cos \theta_i, \sin \theta_i)^\top \in \mathbb{S}^1$ with $\theta_i \in (-\pi, \pi]$ for $i = 0, \dots, n$.

In the method described below, the fundamental step of the construction consists in fitting a circle to a pair of neighboring points and associated normals. The newly generated points are then picked from it. The normal is determined as an appropriately oriented normal of the segment formed by those neighboring points. In each step, the total number of points is (roughly) doubled.

For any vector $\vec{\mathbf{n}} = (n_x, n_y)$, let $\vec{\mathbf{n}}^\perp =$

$r(-n_y, n_x)$ be the vector obtained by a rotation of 90° .

III. FUNDAMENTAL CONSTRUCTION STEP

Consider two points $\mathbf{a}, \mathbf{b} \in \mathbb{R}^2$, $\mathbf{a} \neq \mathbf{b}$ with associated normals $\vec{\mathbf{n}}_{\mathbf{a}}, \vec{\mathbf{n}}_{\mathbf{b}} \in \mathbb{S}^1$. We assume that $\|\mathbf{a} - \mathbf{b}\| = 2r$, where $r > 0$. We construct a circle

$$f(x, y) = 0 \quad (1)$$

where

$$f(x, y) = a(x^2 + y^2) + bx + cy + d, \quad a, b, c, d \in \mathbb{R} \quad (2)$$

which minimizes the objective function

$$F(a, b, c, d) = f(\mathbf{a})^2 + f(\mathbf{b})^2 + \|\nabla f(\mathbf{a}) - \vec{\mathbf{n}}_{\mathbf{a}}\|^2 + \|\nabla f(\mathbf{b}) - \vec{\mathbf{n}}_{\mathbf{b}}\|^2. \quad (3)$$

Hence, the task is to solve

$$\min_{a, b, c, d \in \mathbb{R}} F(a, b, c, d). \quad (4)$$

Clearly, the solution of (4) is invariant with respect to Euclidean transformations. Therefore, we suppose the following choice of the coordinate system (see Figure 1)

$$\mathbf{a} = (-r, 0)^\top, \quad \mathbf{b} = (r, 0)^\top \quad (5)$$

and

$$\vec{\mathbf{n}}_{\mathbf{a}} = (\cos \theta, \sin \theta)^\top, \quad \vec{\mathbf{n}}_{\mathbf{b}} = (\cos \phi, \sin \phi)^\top \quad (6)$$

for $\theta, \phi \in (-\pi, \pi]$. Similarly, all angles will be considered in this interval. Hence, $\frac{\theta}{2} \in (-\frac{\pi}{2}, \frac{\pi}{2}]$.

Note that – using a Euclidean similarity transformation (rigid body motion plus scaling) – any two non-identical points with associated normals can be mapped to this situation. Clearly, the length of the normals may change; it has to be renormalized after the mapping.

Let

$$\alpha = \frac{\theta + \phi}{2} \quad \text{and} \quad \beta = \frac{\theta - \phi}{2} \quad (7)$$

The angles in (7) will be often referred to as functions

$$\alpha(\mathbf{a}, \mathbf{b}, \vec{\mathbf{n}}_{\mathbf{a}}, \vec{\mathbf{n}}_{\mathbf{b}}) \quad \text{and} \quad \beta(\mathbf{a}, \mathbf{b}, \vec{\mathbf{n}}_{\mathbf{a}}, \vec{\mathbf{n}}_{\mathbf{b}}) \quad (8)$$

of the given data.

The following lemma shows that the circle fit exists always, except for pathological cases.

Lemma III.1

- (i) *The problem (4) has a unique solution.*
- (ii) *Let*

$$Z(f) = \{\mathbf{x} \in \mathbb{R}^2: f(\mathbf{x}) = 0\} \quad (9)$$

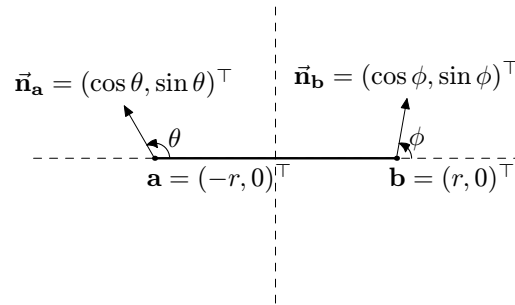


Fig. 1: Local coordinates for analyzing the circle fit (Lemma III.1)

be the zero set of the solution of (4). The set (9) is a real conic section unless $\theta = -\phi = \frac{\pi}{2} + k\pi$ for $k \in \mathbb{Z}$. Moreover, if $\theta = \phi + 2k\pi$ or $\theta = -\phi + 2k\pi$ it is a double line. Otherwise it is a circle.

Proof: The minimization of the function (3) can be done by solving of the 4×4 linear (inhomogeneous) system given by Jacobi matrix

$$\frac{\partial F(a, b, c, d)}{\partial(a, b, c, d)} = \vec{\mathbf{0}}. \quad (10)$$

One can easily check that the coefficient matrix has a non-zero determinant.

Now consider the set (9). Solving the system (10), we get

$$a = \frac{\cos \theta - \cos \phi}{4}, \quad b = \frac{\cos \theta + \cos \phi}{4}, \quad (11)$$

$$c = \frac{\sin \theta + \sin \phi}{2}, \quad d = -\frac{(\cos \theta - \cos \phi)}{4}.$$

The coefficient a vanishes iff

$$\cos \theta - \cos \phi = 0. \quad (12)$$

This condition is equivalent to

$$\theta = \phi + 2k\pi \quad (13)$$

or

$$\theta = -\phi + 2k\pi \quad \text{for } k \in \mathbb{Z}. \quad (14)$$

Clearly, the coefficient d vanishes as well, if (12) holds. In the first case (13), either the coefficient $b \neq 0$ or $c \neq 0$, depending on the angles α and β . Therefore, the solution is a line

$$bx + cy = 0. \quad (15)$$

In the second case (14), we get the non-trivial solution unless the angles $\theta = \frac{\pi}{2} + k\pi$ and $\phi = -\frac{\pi}{2} + k\pi$, since then at least the coefficient $b \neq 0$.

If $a \neq 0$, the solution is a circle. The radius of the circle is

$$r_f = \sqrt{D_f} \quad \text{with} \quad D_f = \frac{b^2 + c^2 - 4ad}{4a^2}. \quad (16)$$

Clearly, there exists a real point on the circle if and only if

$$D_f \geq 0. \quad (17)$$

The case $D_f = 0$ represents a singular real solution – a point.

Substituting the solution (11) into the numerator of (17) and using trigonometric identities, we get an expression discriminating the existence of a real solution

$$\sin^2 \alpha + \frac{1}{(r^2 + 1)^2} \cos^2 \alpha \cos^2 \beta \geq 0. \quad (18)$$

Clearly, it is always non-negative. Moreover, the strict inequality condition holds iff $\theta \neq \frac{\pi}{2} + k\pi$ or $\phi \neq -\frac{\pi}{2} + k\pi$ for any $k \in \mathbb{Z}$. Thus, we get a real circle in the generic case. ■

Assuming $Z(f)$ is a circle, the newly generated point is taken from

$$l \cap Z(f), \quad (19)$$

where the line l is the bisector of the points \mathbf{a} and \mathbf{b}

$$l: \mathbf{x} = \frac{1}{2}\mathbf{a} + \frac{1}{2}\mathbf{b} + t(\mathbf{b} - \mathbf{a})^\perp, \quad t \in \mathbb{R}. \quad (20)$$

Using the choice of coordinates from Figure 1, it is the y -axis (see also Figure 2). After a short calculation, the new point turns out to be one of the two possible solutions

$$\mathbf{q} = \left(0, -r \frac{\cos \beta + 1}{\sin \beta} \right)^\top \quad (21)$$

and

$$\mathbf{q}' = \left(0, -r \frac{\cos \beta - 1}{\sin \beta} \right)^\top. \quad (22)$$

Clearly, the distance of each of the possible new points to the points \mathbf{a} , \mathbf{b} is the same (due to the choice of line l) and we get

$$\|\mathbf{q}' - \mathbf{a}\|^2 = \|\mathbf{q}' - \mathbf{b}\|^2 = \frac{r^2}{\sin^2 \frac{\beta}{2}} \quad (23)$$

and

$$\|\mathbf{q} - \mathbf{a}\|^2 = \|\mathbf{q} - \mathbf{b}\|^2 = \frac{r^2}{\cos^2 \frac{\beta}{2}}. \quad (24)$$

We expect the new point to be in the vicinity of the existing ones. For neighboring points, β is expected to be small. Consequently, we choose the point \mathbf{q} as the appropriate one.

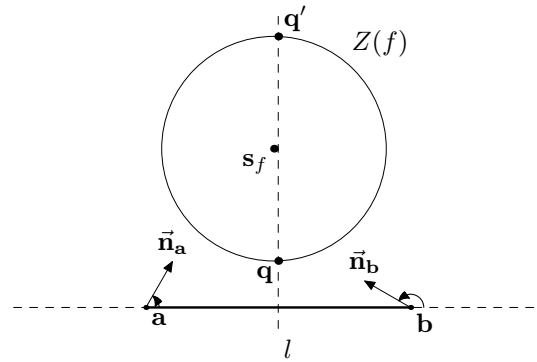


Fig. 2: A new point generated from the fitted circle $Z(f)$ and the line l .

If $Z(f) = \emptyset$ or the intersection of l and $Z(f)$ (see (13) and (14)) contains more than finite number of points, we set

$$\mathbf{q} = \frac{1}{2}\mathbf{a} + \frac{1}{2}\mathbf{b} \quad (25)$$

Next, we need to determine an appropriate normal $\vec{\mathbf{n}}_{\mathbf{q}}$ associated with the new point \mathbf{q} . We assume that the normals $\vec{\mathbf{n}}_{\mathbf{a}}$ and $\vec{\mathbf{n}}_{\mathbf{b}}$ point to the same halfplane of the line $\mathbf{a}\mathbf{b}$. We take the normal of that line pointing in the same halfplane. This choice is invariant under all Euclidean transformations (not only special ones)¹.

Note that the normal can be calculated as an appropriately oriented normal of the circle passing through the points \mathbf{a} , \mathbf{b} , \mathbf{q} , when they are non-collinear due to (24). Hence, the construction will reproduce circles.

Summarizing, we have the following

Algorithm 1 (New Point and Normal) Given two points \mathbf{a} , \mathbf{b} and two associated (unit) normals $\vec{\mathbf{n}}_{\mathbf{a}}$, $\vec{\mathbf{n}}_{\mathbf{b}}$.

If $\langle \vec{\mathbf{n}}_{\mathbf{a}}, \vec{\mathbf{n}}_{\mathbf{b}} \rangle > -1$, compute the new point from

$$\mathbf{q} = \frac{1}{2}\mathbf{a} + \frac{1}{2}\mathbf{b} - \frac{1}{2} \tan \frac{\beta}{2} (\mathbf{b} - \mathbf{a})^\perp \quad (26)$$

where β is given by (7) and the corresponding normal as

$$\vec{\mathbf{n}}_{\mathbf{q}} = \pm \frac{(\mathbf{b} - \mathbf{a})^\top}{\|\mathbf{b} - \mathbf{a}\|} \quad (27)$$

such that $\langle \vec{\mathbf{n}}_{\mathbf{q}}, \vec{\mathbf{n}}_{\mathbf{a}} \rangle > 0$ and $\langle \vec{\mathbf{n}}_{\mathbf{q}}, \vec{\mathbf{n}}_{\mathbf{b}} \rangle > 0$. We denote these functions as $\mathbf{q}(\mathbf{a}, \mathbf{b}, \vec{\mathbf{n}}_{\mathbf{a}}, \vec{\mathbf{n}}_{\mathbf{b}})$ and $\vec{\mathbf{n}}(\mathbf{a}, \mathbf{b}, \vec{\mathbf{n}}_{\mathbf{a}}, \vec{\mathbf{n}}_{\mathbf{b}})$.

¹Another choice would be to use simply the normalized vector $(\mathbf{b} - \mathbf{a})^\top$. This works for all configurations of data, but it is not invariant under reflections.

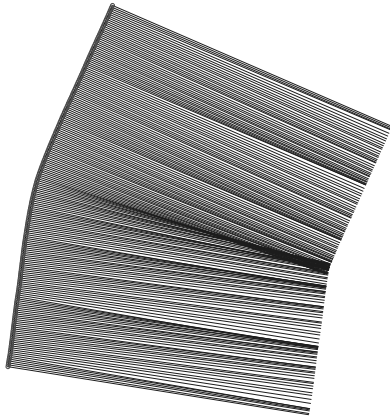


Fig. 4: Zoom of the behavior of the normal for the Figure 3, (ix)

Lemma III.2 *The choice of the new point and the new normal in Algorithm 1 is invariant under the group of Euclidean similarities (including rigid body transformations and scaling) of the plane.*

Proof: The proof of invariance is obvious from (26) and (27). ■

An example of the iteration of the refinement process can be seen in the Figure 3. Starting with set of points and normals shown in part (i), it shows eight iterations of the refinement. Figure 4 shows a closer look at the behavior of the generated normals after the eighth iteration.

IV. ALGEBRAIC SUBDIVISION OF CURVE

After introducing the notation and basic algorithm to refine a polygon, we will now prove some properties of the generated sequence of points. Let

$$P^0 = \{\mathbf{p}_0^0, \dots, \mathbf{p}_{n_0}^0\} \quad (28)$$

and

$$V^0 = \{\bar{\mathbf{n}}_0^0, \dots, \bar{\mathbf{n}}_{n_0}^0\} \quad (29)$$

be the sequence of associated normals with the points in P^0 for $n_0 \in \mathbb{Z}$, $n_0 > 0$. Using Algorithm 1, we obtain iteratively a system of sequences

$$P^j = \{\mathbf{p}_0^j, \dots, \mathbf{p}_{n_j}^j\} \quad (30)$$

and

$$V^j = \{\bar{\mathbf{n}}_0^j, \dots, \bar{\mathbf{n}}_{n_j}^j\} \quad (31)$$

such that

$$\mathbf{p}_{2k+1}^{j+1} = \mathbf{q}(\mathbf{p}_k^j, \mathbf{p}_{k+1}^j, \bar{\mathbf{n}}_k^j, \bar{\mathbf{n}}_{k+1}^j) \quad (32)$$

for $j = 0, 1, 2, \dots$, $k = 0, \dots, n_{j-1} - 2$,

$$\mathbf{p}_{2k}^{j+1} = \mathbf{p}_k^j \quad (33)$$

for $j = 0, 1, 2, \dots$, $k = 0, \dots, n_{j-1} - 1$, are the newly generated points and

$$\bar{\mathbf{n}}_{2k+1}^{j+1} = \bar{\mathbf{n}}(\mathbf{p}_k^j, \mathbf{p}_{k+1}^j, \bar{\mathbf{n}}_k^j, \bar{\mathbf{n}}_{k+1}^j) \quad (34)$$

for $j = 0, 1, 2, \dots$, $k = 0, \dots, n_{j-1} - 2$,

$$\bar{\mathbf{n}}_{2k}^{j+1} = \bar{\mathbf{n}}_k^j, \quad (35)$$

for $j = 1, 2, \dots$, $k = 0, \dots, n_{j-1} - 1$ are the newly generated vectors associated with the corresponding points, where

$$n_{j+1} = 2n_j \quad (36)$$

for $j = 0, 1, 2, \dots$

Associated with the sequences (30) and (31), we have also the sequences of local angles

$$\{\theta_i^j\}_{i=0}^{n_j-1} \quad \text{and} \quad \{\phi_i^j\}_{i=0}^{n_j-1} \quad (37)$$

such that

$$\bar{\mathbf{n}}_i^j = (\cos \theta_i^j, \sin \theta_i^j)^\perp \quad (38)$$

and

$$\bar{\mathbf{n}}_{i+1}^j = (\cos \phi_i^j, \sin \phi_i^j)^\perp \quad (39)$$

in local coordinate system determined by the points $\mathbf{p}_i^j, \mathbf{p}_{i+1}^j$ (see Figure 1). Using (7), we also have an equivalent description

$$\{\alpha_i^j\}_{i=0}^{n_j-1} \quad \text{and} \quad \{\beta_i^j\}_{i=0}^{n_j-1} \quad (40)$$

of the parameter angles for $j = 0, 1, 2, \dots$, where

$$\alpha_i^j = \alpha(\mathbf{p}_i^j, \mathbf{p}_{i+1}^j, \bar{\mathbf{n}}_i^j, \bar{\mathbf{n}}_{i+1}^j) \quad (41)$$

and

$$\beta_i^j = \beta(\mathbf{p}_i^j, \mathbf{p}_{i+1}^j, \bar{\mathbf{n}}_i^j, \bar{\mathbf{n}}_{i+1}^j). \quad (42)$$

Note, that the angles α_i^j and β_i^j are also considered in the local coordinate systems defined by the neighboring points. Clearly, we may consider the sequences (30), (31) as sets and then

$$P^j \subset P^{j+1} \quad \text{and} \quad V^j \subset V^{j+1} \quad (43)$$

for $j = 0, 1, 2, \dots$. Let

$$P^\infty = \bigcup_{j=0}^{\infty} P^j \quad \text{and} \quad V^\infty = \bigcup_{j=0}^{\infty} V^j \quad (44)$$

be the limit set of the generated points resp. vectors. We prove several properties of these sets.

Each of the sequences P^j defines a polygon in \mathbb{R}^2 . We denote it with $\text{poly}(P^j)$. It can be piecewise linearly parameterized. For P^0 , we use

$$\mathbf{p}^0(t) = \frac{t_{i+1} - t}{t_{i+1} - t_i} \mathbf{p}_i^0 + \frac{t - t_i}{t_{i+1} - t_i} \mathbf{p}_{i+1}^0 \quad (45)$$

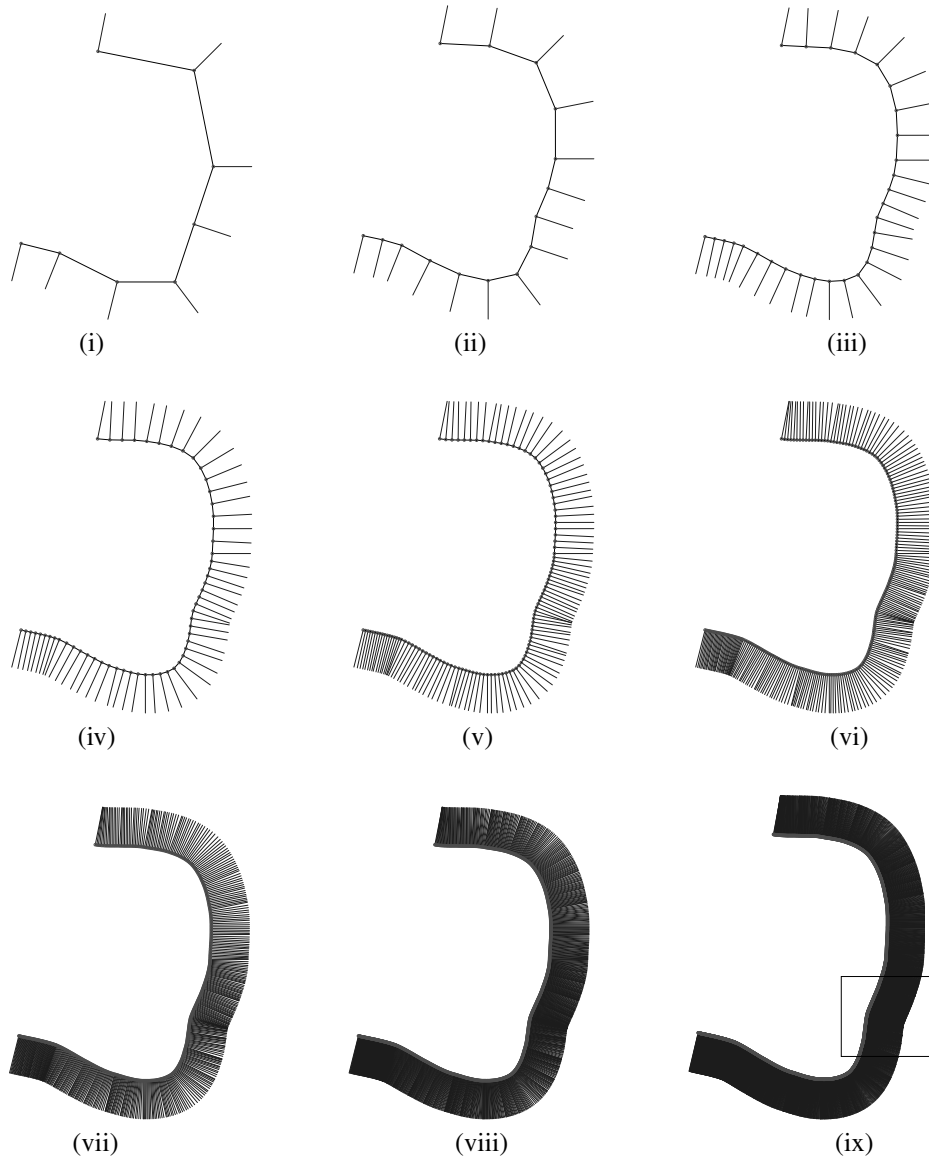


Fig. 3: The sequence of eight subdivision steps for refining the data given in the part (i). The behavior in part (ix) is shown in Figure 4

for $t \in [t_i, t_{i+1}]$, where $t_i = i$ for $i = 0, 1, \dots, n_0$. Now, we can continue inductively with the parameterization of $\text{poly}(P^j)$ as

$$\mathbf{p}^j(t) = 2^j(t - t_i^j)\mathbf{p}_i^j + 2^j(t_{i+1}^j - t)\mathbf{p}_{i+1}^j \quad (46)$$

for $t \in [t_i^j, t_{i+1}^j]$, where $t_i^j = \frac{i}{2^j}$ for $i = 0, 1, \dots, n_j$. The parameters t_i^j are called dyadic knots. Note, that due to (33)

$$\mathbf{p}^{j+1}(t_{2i}^{j+1}) = \mathbf{p}^j(t_i^j) \quad (47)$$

for $j = 0, 1, \dots; i = 0, 1, \dots, n_j$. Similarly, we parameterize the corresponding vector function as

$$\bar{\mathbf{n}}^j(t) = 2^j(t - t_i^j)\bar{\mathbf{n}}_i^j + 2^j(t_{i+1}^j - t)\bar{\mathbf{n}}_{i+1}^j \quad (48)$$

for $t \in [t_i^j, t_{i+1}^j]$.

Once we have accomplished this, we can consider the sequence (40) as a sequence of piecewise constant functions, each defined on the interval $[0, n_0]$ with uniform binary refinement (see Figure 5).

Clearly, the values $\mathbf{p}(t_i^j)$ of the set P^∞ and $\bar{\mathbf{n}}(t_i^j)$ of the set V^∞ depend locally on the initial values. Hence, it suffices to consider a pair of neighboring points and normals to reveal local properties of the generated sets.

In the sequel we assume that

$$\langle \bar{\mathbf{n}}_i^j, \bar{\mathbf{n}}_{i+1}^j \rangle > -1 \quad (49)$$

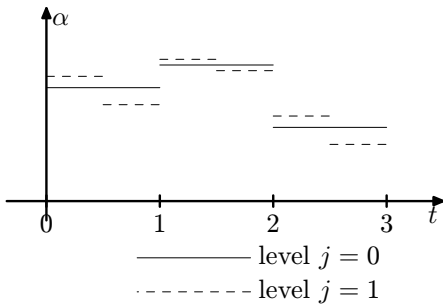


Fig. 5: Change of the step function α during the refinement over the parameterization interval $[0, n_0]$ for $n_0 = 4$.

holds for $j = 0, 1, \dots, i = 0, \dots, n_j - 1$.

V. PROPERTIES OF ALGEBRAIC SUBDIVISION CURVE SEGMENT

Consider the set $P^0 = \{\mathbf{a}, \mathbf{b}\}$ for $\mathbf{a} \neq \mathbf{b}$ as in (5) and $V^0 = \{\vec{\mathbf{n}}_{\mathbf{a}}, \vec{\mathbf{n}}_{\mathbf{b}}\}$ as defined in (6). Hence, $n_0 = 1$ in this section.

We will prove that the generated set P^∞ is a dense subset of G^1 curve and, moreover, the normals of that curve are those in V^∞ for the corresponding points.

The proof consists of the following steps.

- 1) First, we prove the technical Lemma V.1, which preserves certain configurations of data during the subdivision.
- 2) Second, we show that the polygons generated by our algorithm are convex, provided the initial data are in certain configurations, and form a Cauchy sequence in $C^0[0, 1]$ space with maximum norm.
- 3) As the last step, we show that the limit of that sequence of C^0 functions is in fact G^1 , by considering the existence of tangent in each generated point.

The following technical lemma is a key tool for the proof of the properties of the limit sets (44).

Lemma V.1 *If the following conditions*

$$\beta_0^0 > 0 \quad (50)$$

$$0 < \alpha_0^0 \leq \frac{\pi}{2} \quad (51)$$

$$-\frac{\beta_0^0}{2} < \alpha_0^0 - \frac{\pi}{2} \quad (52)$$

hold for P^0 and V^0 , then the similar conditions

$$\beta_i^j > 0 \quad (53)$$

$$0 < \alpha_i^j \leq \frac{\pi}{2} \quad (54)$$

$$-\frac{\beta_i^j}{2} < \alpha_i^j - \frac{\pi}{2} \quad (55)$$

hold in P^j and V^j for $j = 0, 1, \dots, i = 0, 1, \dots, n_j - 1$.

As a geometrical interpretation, the conditions of this lemma are satisfied in the gray region on the Figure 6.

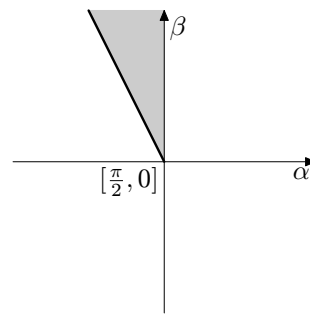


Fig. 6: Area of parameters for the Lemma V.1

Proof: We prove the statement by induction on j . Clearly, for $j = 0$

$$\alpha_0^0 - \frac{\pi}{2} < \frac{\beta_0^0}{2} \quad (56)$$

$$\frac{\beta_0^0}{2} < \alpha_0^0 + \beta_0^0 \quad (57)$$

and

$$\alpha_0^0 - \beta_0^0 < \pi - \frac{\beta_0^0}{2}, \quad (58)$$

see Figure 7, where indices of α and β were omitted in order to simplify the figure.

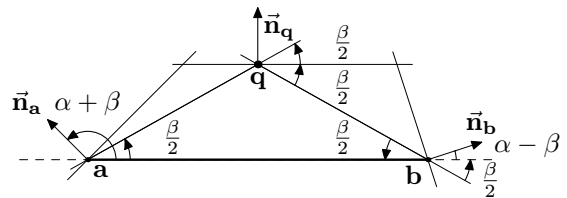


Fig. 7: Angles in a subdivision step

Then, the new angles in the local coordinates determined by points \mathbf{a}, \mathbf{q} are $\theta_0^1 = \alpha_0^0 + \frac{\beta_0^0}{2}$ and $\phi_0^1 = \frac{\pi}{2} - \frac{\beta_0^0}{2}$. Similarly, $\theta_1^1 = \frac{\pi}{2} + \frac{\beta_0^0}{2}$ and $\phi_1^1 = \alpha_0^0 + \frac{\beta_0^0}{2}$ are angles for the coordinate system determined by points \mathbf{q}, \mathbf{b} . After a short calculation, using (7), we get

and

$$l_i^j : \langle (\mathbf{x} - \mathbf{p}_i^j), \bar{\mathbf{n}}_i^j \rangle = 0. \quad (73)$$

Clearly, the new polygon is again locally convex. Due to the convexity of the poly(P^j), we can find a point \mathbf{x}^j such that each newly generated point lies in the wedge $\mathbf{p}_i^j \mathbf{x}^j \mathbf{p}_{i+1}^j$ (see Figure 9). Hence, the polygon poly(P^{j+1}) has no self-intersections and, therefore, is also convex. ■

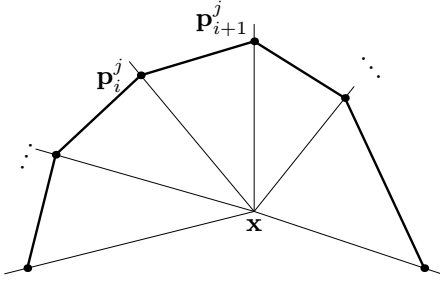


Fig. 9: Splitting of a convex polygon into wedges

Corollary V.1 *The inequality*

$$\min_{\substack{i, k \in \{0, \dots, n_j\} \\ i \neq k}} \|\mathbf{p}_i^j - \mathbf{p}_k^j\| > 0 \quad (74)$$

holds for every $j = 0, 1, \dots$

The result of the previous corollary means that we generate a sequence in each refinement step, where no two points are identical.

Lemma V.3 *If the conditions (50), (51), (52), (64) and (65) hold, the sequence of polygons*

$$\{\mathbf{p}^j(t)\}_{j=0}^\infty \quad (75)$$

converges to a convex C^0 curve.

Proof: The assumptions and Lemma V.2 imply that we get a convex polygon $\mathbf{p}^j(t)$ in each step of the refinement. Considering the parameterization (46) and using (24), we get

$$\|\mathbf{p}^{j+1}(t) - \mathbf{p}^j(t)\| \leq r_{\max}^j \frac{1}{\cos \frac{\beta_{\max}^j}{2}}, \quad (76)$$

for sufficiently large j , where

$$r_{\max}^j = \frac{1}{2} \max_{i=0, \dots, n_j-1} \|\mathbf{p}_{i+1}^j - \mathbf{p}_i^j\| \quad (77)$$

and

$$\beta_{\max}^j = \max_{i=0, \dots, n_j-1} |\beta_i^j|. \quad (78)$$

Using (24), we get

$$r_{\max}^{j+1} \leq \frac{1}{2 |\cos \frac{\beta_{\max}^j}{2}|} r_{\max}^j. \quad (79)$$

By induction using (59), (60) and (61), we get

$$|\beta_i^j| \leq \frac{|\beta_0^0|}{2^j} + \frac{j |\alpha_0^0 - \frac{\pi}{2}|}{2^j}. \quad (80)$$

Clearly, $\beta_{\max}^j \rightarrow 0$ as $j \rightarrow \infty$. Hence, there is a constant D , $0 < D < 1$ and an integer $j_0 \in \mathbb{Z}_+$ such that

$$0 < \frac{1}{2 |\cos \frac{\beta_{\max}^j}{2}|} < D < 1 \quad (81)$$

holds for all $j > j_0$. Summing up,

$$\|\mathbf{p}^{j+1}(t) - \mathbf{p}^j(t)\| \leq 2r_{\max}^j D^{j+1} \quad (82)$$

for $j > j_0$ and therefore (75) is a Cauchy sequence of globally bounded C^0 convex polygons. Therefore, it converges uniformly to a convex C^0 curve. ■

Corollary V.2 *The sequence of vector functions*

$$\{\bar{\mathbf{n}}^j(t)\}_{j=0}^\infty \quad (83)$$

converges to a continuous vector function $\bar{\mathbf{n}}(t)$ along the curve $\mathbf{p}(t)$.

Proof: Applying (80), we get the result. ■

Now, we need to prove the existence of tangent for each generated point in P^∞ . We consider the sequences of the points in P^∞ . We use the local coordinate system described in Section II, see Figure 1. Such a coordinate system exists, iff the considered points are distinct. Corollary V.1 proves the existence of such local coordinate system for any two generated points.

Lemma V.4 *If the conditions (50), (51) and (52) hold, the system of sequences (40) has the following properties:*

- 1) For $k = 0, 1, \dots, j = 0, 1, \dots, i = 0, \dots, n_j - 1$

$$\alpha_i^j - \frac{\pi}{2} = \sum_{l=2^k i}^{2^k(i+1)-1} \left(\alpha_l^{j+k} - \frac{\pi}{2} \right) \quad (84)$$

$$\beta_i^j = \sum_{l=2^k i}^{2^k(i+1)-1} \beta_l^{j+k} \quad (85)$$

- 2) Let $\{\mathbf{q}_k\}_{k=0}^\infty$ be a convergent sequence of points $\mathbf{q}_k = \mathbf{p}_{i_k}^{j_k} \in P^\infty$ and $\lim_{k \rightarrow \infty} \mathbf{q}_k = \mathbf{q}$, where $\mathbf{q} = \mathbf{p}_I^J$, for some $J \in \mathbb{Z}_+$ and $I \in \{0, \dots, n_j\}$. Suppose, $\mathbf{q}_k \neq \mathbf{q}$ for any $k \in \mathbb{Z}_+$. Then

$$\lim_{j \rightarrow \infty} \alpha(\mathbf{q}_k, \mathbf{q}, \bar{\mathbf{n}}_{\mathbf{q}_k}, \bar{\mathbf{n}}_{\mathbf{q}}) = \frac{\pi}{2} \quad (86)$$

$$\lim_{j \rightarrow \infty} \beta(\mathbf{q}_k, \mathbf{q}, \bar{\mathbf{n}}_{\mathbf{q}_k}, \bar{\mathbf{n}}_{\mathbf{q}}) = 0. \quad (87)$$

Proof: The (84) and (85) can be proven by induction using (59), (60) and (61).

For the second part, we can assume without loss of generality that $\mathbf{q} = \mathbf{p}_0^0$. Further, let $\{t_k\}_{k=0}^\infty$ be the sequence of the dyadic parameters corresponding to $\{\mathbf{q}_k\}$. Since the limit curve $\overline{P^\infty}$ is convex, we have $t_k \rightarrow 0$.

First, we prove the second part for special sequences. Let $\mathbf{q}_k = \mathbf{p}_{i_k}^k$ be such that $i_{k+1} = 2i_k$ or $i_{k+1} = 2i_k + 1$ for $k = 0, \dots$. Then $\alpha(\mathbf{q}_k, \mathbf{q}, \vec{\mathbf{n}}_{\mathbf{q}_k}, \vec{\mathbf{n}}_{\mathbf{q}}) = \alpha_{i_k}^k$ for $k = 0, 1, \dots$. Using (59), we get (86) by induction. Similarly, $\beta(\mathbf{q}_k, \mathbf{q}, \vec{\mathbf{n}}_{\mathbf{q}_k}, \vec{\mathbf{n}}_{\mathbf{q}}) = \beta_{i_k}^k$ and using (80), we get (87) for the special case.

Now, let the sequence $\{\mathbf{q}_k\}_{k=0}^\infty$ of points be arbitrary. Let $t_k = \frac{i_k}{2^{m_k}}$. Then, using (51) and (84), we have

$$\begin{aligned} 0 &\geq \alpha(\mathbf{q}_k, \mathbf{q}, \vec{\mathbf{n}}_{\mathbf{q}_k}, \vec{\mathbf{n}}_{\mathbf{q}}) - \frac{\pi}{2} \\ &= \sum_{l=0}^{l_k} \left(\alpha_l^{i_k} - \frac{\pi}{2} \right) \geq \alpha_0^{m_k} - \frac{\pi}{2}, \end{aligned} \quad (88)$$

for some $l_k \in \{0, \dots, m_k - 2\}$ and

$$m_k = \max\{m \in \mathbb{Z}_+; 2^{-m} > t_k\}. \quad (89)$$

Since $t_k \rightarrow 0$ for $m_k \rightarrow \infty$, using (86) for the special case proved above, we get the convergence in general case.

In order to prove (87) in the general case, we have via (50) and (85)

$$0 \leq \beta(\mathbf{q}_k, \mathbf{q}, \vec{\mathbf{n}}_{\mathbf{q}_k}, \vec{\mathbf{n}}_{\mathbf{q}}) = \sum_{l=0}^{l_k} \beta_l^{i_k} \leq \beta_0^{m_k}. \quad (90)$$

Using (87) for the special case, we get the result for all sequences. ■

The last step is the proof of G^1 continuity of the limit curve. Since we know the curve is C^0 according to the Lemma V.3, we prove the existence of the tangent line for every generated points. The normal of this line will be the corresponding generated normal vector at the point.

Lemma V.5 *If the conditions (50), (51), (52), (64) and (65) hold, then the set $\overline{P^\infty}$ is a convex curve with a well defined tangent and is therefore G^1 everywhere.*

Proof: Let $\{\mathbf{q}_k\}_{k=0}^\infty$ be a convergent sequence of points in P^∞ and $\mathbf{q}_k \rightarrow \mathbf{q} \in P^\infty$. Let the unit normal of the line $\overline{\mathbf{q}\mathbf{q}_k}$ be denoted as $\vec{\mathbf{m}}_k$. We prove, that $\vec{\mathbf{m}}_k \rightarrow \vec{\mathbf{n}}_{\mathbf{q}}$ as $k \rightarrow \infty$. In order to

prove this, we prove the convergence of the angles between the vectors $\vec{\mathbf{m}}_k$ and $\vec{\mathbf{n}}_{\mathbf{q}}$ converges to 0,

$$\lim_{k \rightarrow \infty} \left\langle \frac{\mathbf{q}_k - \mathbf{q}}{\|\mathbf{q}_k - \mathbf{q}\|}, \vec{\mathbf{n}}_{\mathbf{q}} \right\rangle = 0. \quad (91)$$

Since the function $\vec{\mathbf{n}}(t)$ is continuous according to Corollary V.2, we suppose, that $\vec{\mathbf{m}}_k$ is in a the neighborhood of $\vec{\mathbf{n}}_{\mathbf{q}}$. Let $\{\alpha_k\}_{k=0}^\infty$ and $\{\beta_k\}_{k=0}^\infty$ be the sequences, where

$$\alpha_k = \alpha(\mathbf{q}_k, \mathbf{q}, \vec{\mathbf{m}}_k, \vec{\mathbf{n}}_{\mathbf{q}}) \quad (92)$$

and

$$\beta_k = \beta(\mathbf{q}_k, \mathbf{q}, \vec{\mathbf{m}}_k, \vec{\mathbf{n}}_{\mathbf{q}}). \quad (93)$$

Using Lemma V.4 we get (see also Figure 10)

$$\left\langle \frac{\mathbf{q}_k - \mathbf{q}}{\|\mathbf{q}_k - \mathbf{q}\|}, \vec{\mathbf{n}}_{\mathbf{q}} \right\rangle = \cos \delta_k = \cos(\pi - \alpha_k + \beta_k) \rightarrow 0 \quad (94)$$

when $\delta_k > 0$ and similarly

$$\left\langle \frac{\mathbf{q}_k - \mathbf{q}}{\|\mathbf{q}_k - \mathbf{q}\|}, \vec{\mathbf{n}}_{\mathbf{q}} \right\rangle = \cos \delta_k = \cos(\alpha_k + \beta_k) \rightarrow 0 \quad (95)$$

when $\delta_k \leq 0$. This completes the proof for the sequences from P^∞ . Using completion and the fact that $\vec{\mathbf{n}}$ is C^0 , we conclude that the $\overline{P^\infty}$ is locally G^1 with well defined normal in $\overline{V^\infty}$. ■

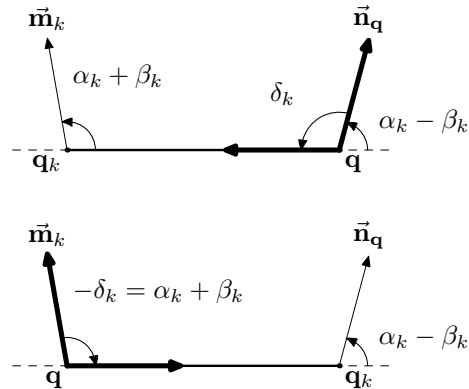


Fig. 10: The convergence of the tangent for positive and negative δ_k

Summing up, we have

Theorem V.1 *Let*

$$0 < \beta_i^0 < \frac{\pi}{4} \quad (96)$$

$$\left| \alpha_i^0 - \frac{\pi}{2} \right| \leq \frac{\pi}{4} \quad (97)$$

$$-\frac{\beta_i^0}{2} < \alpha_i^0 - \frac{\pi}{2} \quad (98)$$

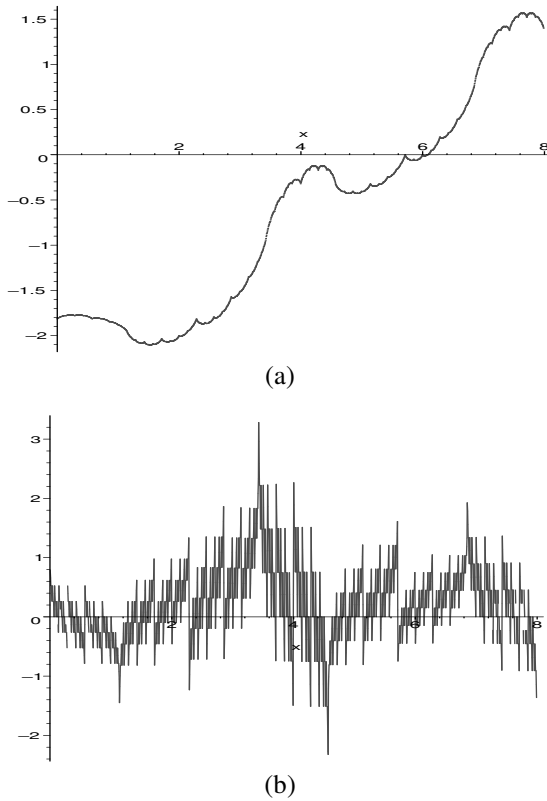


Fig. 11: (a) The graph of the normal angle; (b) Graph of the approximating the curvature of the curve

for $i = 0, \dots, n_0 - 1$. Then the set $\overline{P^\infty}$ is a convex curve with a well defined tangent, hence it is G^1 everywhere.

Note, that the result of Theorem V.1 means, that the generated curve is C^1 after an appropriate reparameterization.

In order to visualize this result, we have checked the quality of the generated curve, as follows. First, we have generated the graph of the normal angle for the generated curve in Figure 3, see Figure 11, (a). Clearly, it is a continuous function of the dyadic parameter.

In Figure 11, (b), the approximation of the curvature (the inverse of the radius of the circle passing through three consecutive generated points) is shown. Both figures are from the level (ix) of the refinement in Figure 3. The limit curve does not seem to have a well-defined curvature.

VI. CONCLUSION AND FUTURE WORK

We have presented a novel method for refinement of the sequence of points in plane associated with a unit normal vectors. The method is invariant

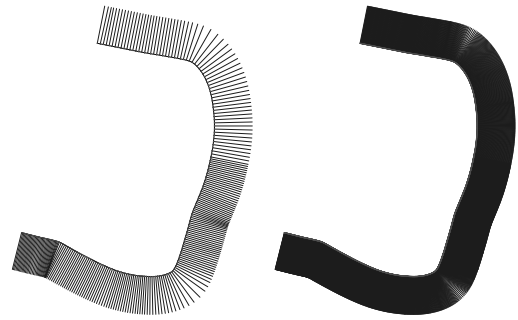


Fig. 12: Smoother normal approximation after 5 and 8 subdivision steps

under Euclidean similarities. It produces a G^1 curve, provided certain conditions are satisfied by the initial data. The initial data (points with associated normals) are interpolated by the generated curve. Since we used circle fits to generate new points, it is clear, that this construction reproduces a circle, if the initial data are taken from the circle.

In order to improve the local behavior of the generated set of points, we have developed an experimental method with smoother normal (see Figure 12). The initial data are taken those from Figure 3, (i). In this case, we fit to the set of four consecutive points and their normals a general conic section. The new point and the corresponding normal are picked from this conic. The construction provides interpolation of the initial points, whereas the normals are adapted during the refinement.

The graph of the normals (see Figure 13, (a)) and the corresponding graph of the curvature radius (see Figure 13, (b)) show a promising behavior. The generated curve and the normal field can be seen on Figure 12. The properties of these curves will be analyzed in the future.

The method can also be extended to the surface case. In this context, we have consider triangular meshes with given normals in the vertices. The new point can be taken as a suitable point picked up from a quadric fitted to certain neighborhood of the triangle.

ACKNOWLEDGMENT

This research was supported by the Austrian Science Funds (FWF) through the SFB F013 “Numerical and Symbolic Scientific Computing” at Linz, project 15.

REFERENCES

- [1] J. Warren, *Subdivision Methods For Geometric Design: A Constructive Approach*. Morgan Kaufmann, 2003.

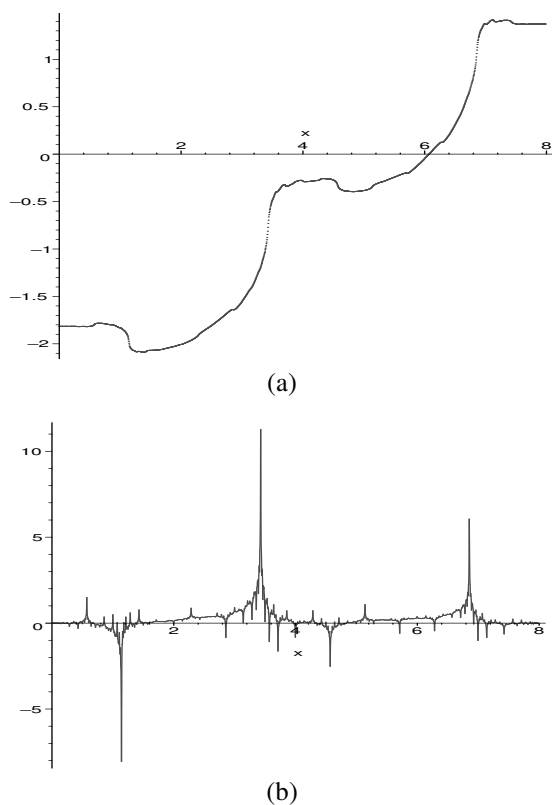


Fig. 13: (a) The graph of the normal angle; (b) Graph of the approximation of the curvature of the curve in Figure 12

- [2] G. Morin, J. Warren, and H. Weimer, "A subdivision scheme for surfaces of revolution." *Comput. Aided Geom. Des.*, vol. 18, no. 5, pp. 483–502, 2001.
- [3] B. Jüttler and U. Schwanecke, "Analysis and design of Hermite subdivision schemes," *The Visual Computer*, vol. 18, pp. 326–342, 2002.
- [4] T. E. Nicolas Aspert and P. Vanderghyest, "Non-linear subdivision using local spherical coordinates," *Comput. Aided Geom. Des.*, vol. 20, no. 3, pp. 165–187, 2003.
- [5] S. Karbacher, S. Seeger, and G. Häusler, "A non-linear subdivision scheme for triangle meshes," in *Proceedings of the 2000 Conference on Vision Modeling and Visualization*, B. Girod *et al.*, Eds. Saarbrücken: Aka GmbH, 2000, pp. 163–170.
- [6] M.-S. Kim and K.-W. Nam, "Interpolating solid orientations with circular blending quaternion curves," *Computer-Aided Design*, vol. 27, no. 5, pp. 385–398, 1995.
- [7] C. H. Séquin, K. Lee, and J. Yen, "Fair, G^2 - and C^2 -continuous circle splines," submitted to CAD 2003.
- [8] D. Parkinson and D. Moreton, "Optimal biarc-curve fitting," *Computer-Aided Design*, vol. 23, no. 6, pp. 411–416, 1991.
- [9] M. Sabin, "A geometry-driven variant of the four-point subdivision scheme," manuscript.